Direct measurements of the masses of rubidium and cesium isotopes far from stability

M. Epherre, G. Audi, C. Thibault, R. Klapisch, G. Huber,* F. Touchard, and H. Wollnik†

*Laboratoire René Bernas du C.S.N.S.M.,Bât. 108, 91406, Orsay, France
and ISOLDE Collaboration, CERN,1211, Geneva, Switzerland*

The masses of neutron-deficient and neutron-rich isotopes of rubidium ($^{74-79}$Rb, $^{90-99}$Rb) and of cesium ($^{117-124,126}$Cs, $^{138,140-147}$Cs) have been determined by direct on-line mass spectrometry. The measured masses are compared to current mass predictions. From the trend of neutron separation energies, experimental neutron pairing energies are deduced and evidence is found for the onset of a deformation at $N = 60$ in the neutron-rich rubidium isotopes.

> NUCLEAR STRUCTURE $^{74-79}$Rb, $^{90-99}$Rb, $^{117-124,126}$Cs,$^{138,140-147}$Cs; measured masses, on-line mass spectrometry. S_{2n} deduced; evidence for deformation at $N = 60$. Comparison with mass predictions.

I. INTRODUCTION

In extending our knowledge of nuclear structure to nuclei far from the stability line, information on ground-state masses is among the most obvious that must be gained. An extensive set of precisely determined masses would allow a more secure prediction of the limits of nuclear stability and permit a better determination of the parameters of nuclear mass formulas that have thus far been adjusted with data from the bottom of the valley.[1] Moreover, binding energy systematics can reveal in a most direct way new features such as deformations or shell closures. A recent example is the case of the sodium isotopes with $N \sim 20$.[2,3]

Usually masses of radioactive nuclei are determined by γ-coincident β-end-point energies, nuclear reaction Q values, and sometimes Q_α values. Direct mass spectrometric techniques, on the other hand, are normally confined to high precision determination of the masses of stable nuclei.[4] In the case of light nuclei ($A \sim 30$), it was shown, however, that with a single stage mass spectrometer one could measure on-line masses of sodium isotopes with a precision of $\sim 3 \times 10^{-6}$ (Ref. 2) (i.e., 100 keV for $A = 30$).

To maintain the same significant accuracy of ~ 100 keV for heavier nuclei ($A \gtrsim 100$) requires a corresponding increase of the precision of the mass determination. This is not possible with single stage mass spectrometers but obviously within the possibilities of conventional "double-focusing" machines.[5] The low transmission which is generally associated with their high resolution has to be compensated by an adequate intensity of radioactive atoms. This is the case for intensities of beams of radioactive ions that are available at the ISOLDE Isotope Separator at CERN for a large number of chemical elements.[6-8]

We have therefore connected a mass spectrometer to ISOLDE in order to initiate a systematic program of mass determinations of the short-lived nuclei available there. We wish to report in this paper on the first extensive series which we have completed for elements Rb and Cs. The extension of our measurements on both sides of the valley of stability is shown on Fig. 1.

The isotopes which we have studied are produced in reactions induced by the 600 MeV protons of the CERN synchrocyclotron. Spallation of niobium and lanthanum produce neutron-deficient isotopes of rubidium and cesium respectively,[6] whereas the neutron-rich isotopes of both elements are produced by fission of uranium (Fig. 2). The system of target, ion source, ion beam acceleration, mass separation, and transport that constitute the ISOLDE facility are described elsewhere.[9]

II. EXPERIMENTAL METHOD

A. Description of the setup

The 60 keV mass separated ions produced by ISOLDE are focused and stopped on the inner face of a conical tantalum tube heated to ~ 1200 °C (see Fig. 3). The implanted atoms diffuse back quickly to the foil surface where they are ionized and the bias from the 3 volt dc heating potential directs them to the entry of a thick lens optical system. This forms a 9 keV ion beam which is focused on the narrow entrance slit S_1 of the mass spectrometer. This instrument has been adapted by us from a commercially available design.[10] It has a modified Mattauch Herzog geometry with the following characteristics: spherical electrostatic analyzer, angle 45°, radius 45 cm; homogeneous magnetic sector, deflection angle 80°, radius 30
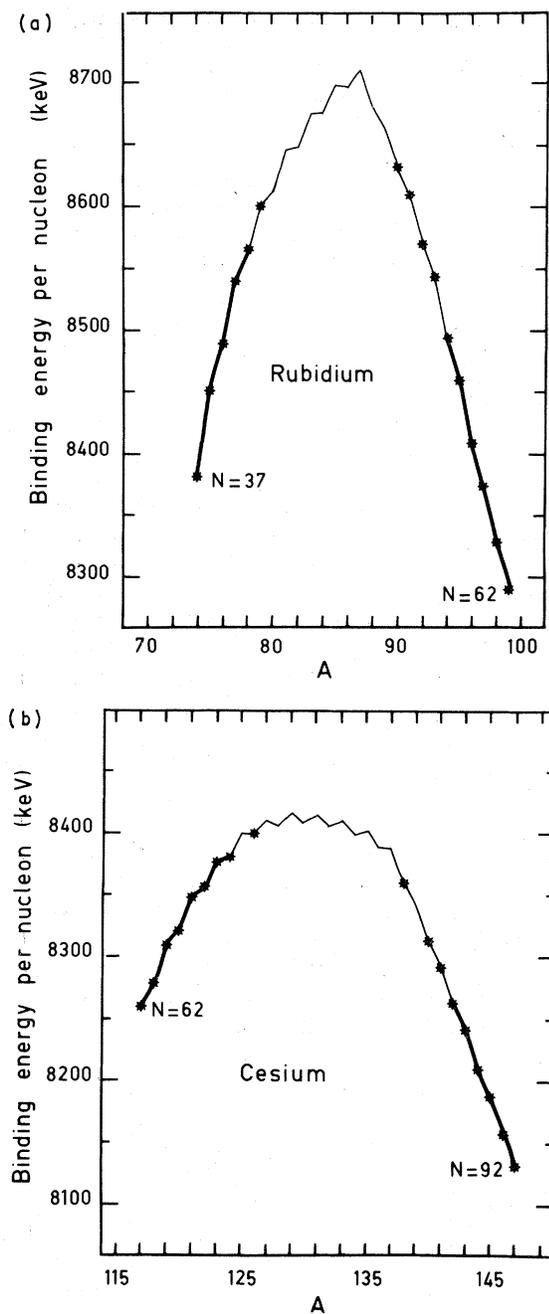
FIG. 1. The new extension of the binding energy parabola (heavy line) brought by the present measurements (stars): (a) rubidium, (b) cesium.

FIG. 2. Production yield curves at ISOLDE for the isotopes we have measured (normalized to 1 μA proton beam). (a) Rubidium isotopes are produced either from a Nb target (solid points) or from a U target (open points). (b) Cesium isotopes are produced either from a La target (solid points) or from a U target (open points).

cm, entrance angle adjustable around 29°, exit angle 29°. The path length is 185 cm.

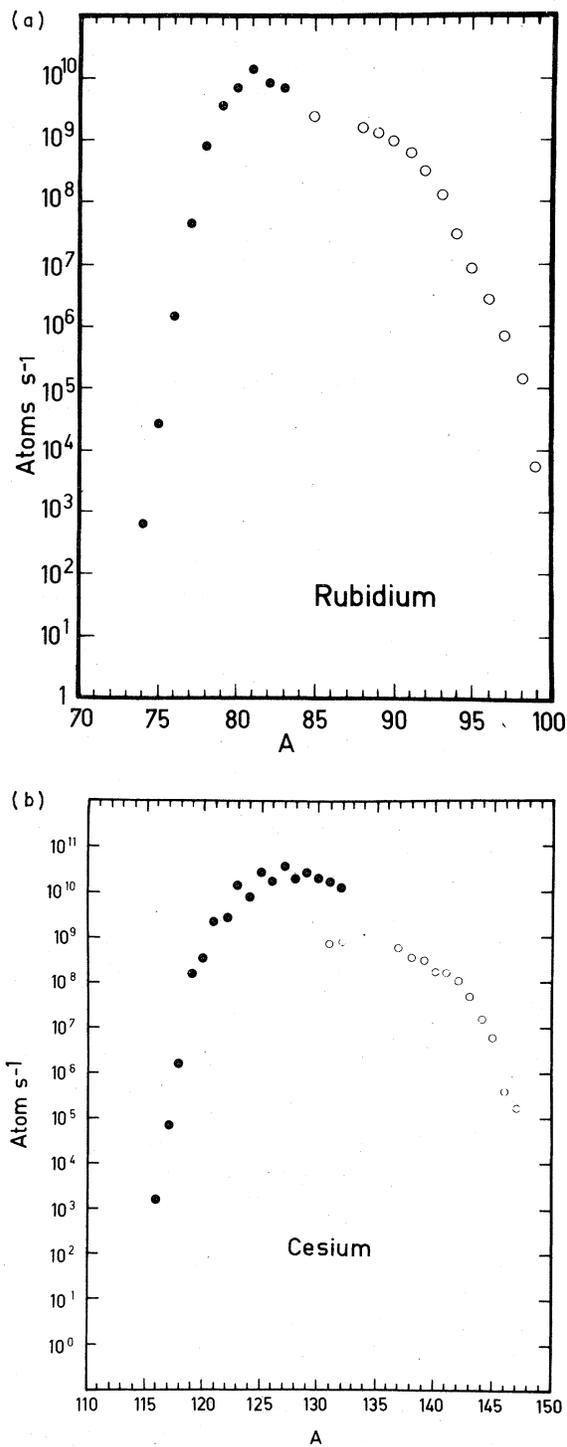This system is known to be focusing in energy and angle (to first order). The ions passing the
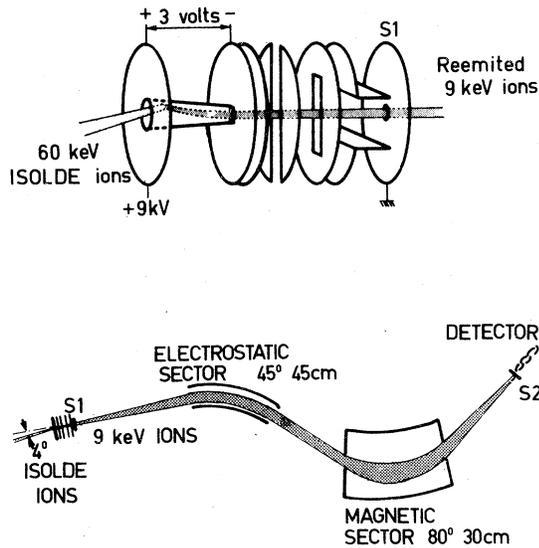
FIG. 3. Schematic view of the experiment. The upper part shows the 60 keV ISOLDE ions stopped in the tantalum tube, the atoms reionized, accelerated to 9 keV and focused through the various lenses of the optical system. The lower part shows the trajectory of the 9 keV ions through the mass spectrometer between the entrance slit S_1 and the exit slit S_2.

slit S_2 are detected by a high gain electron multiplier which counts single ions impinging on the first dynode. To avoid the difficulties created by the high background from the radioactive ions implanted on the first dynode, a special detector where the conversion of ion to electrons takes place on a moving tape has been developed.[11,12]

B. Principle of the measurement

High precision mass measurements are always relative and rest on the well known property[13] that if two ions of masses M_A and M_B follow the same trajectory in the same magnetic field between slits S_1 and S_2 (see Fig. 3) all the potentials, V, U,... of the ion optical system should obey the relation

$$\frac{M_A}{M_B} = \frac{V_B}{V_A} = \frac{U_B}{U_A} = \cdots .$$

Therefore the accelerating potential U and the deflecting potential V have to be kept proportional; the ratio of one of them has to be measured very precisely to determine the ratio of masses. Because of the energy focusing property of the mass spectrometer, the ion trajectory at the exit slit is less sensitive to variations of U than to variations of V so that it is the potential difference V at the electrostatic sector electrodes which one
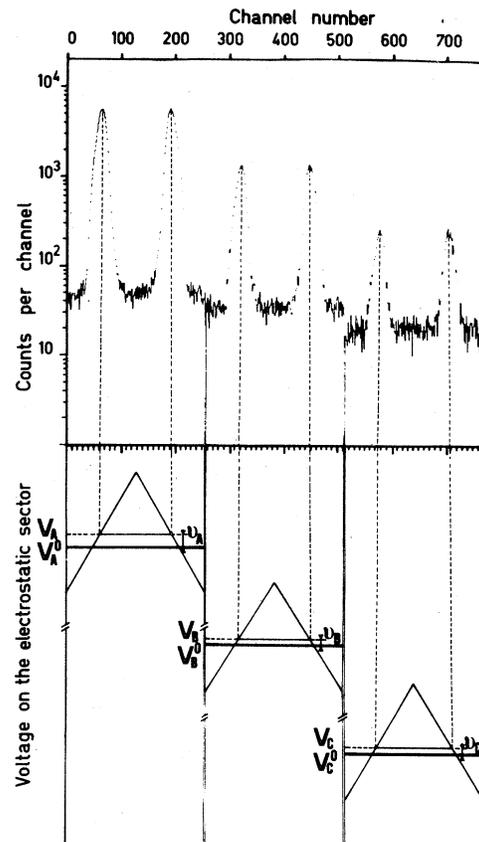

FIG. 4. Spectrum from the multiscaler showing as an example the recording of rubidium isotopes 95, 97, 98 in three different sections. The scheme of the corresponding modulated voltage is shown underneath. Because of the relative abundances of each of the isotopes (^{95}Rb/^{97}Rb ~ 10, ^{95}Rb/^{98}Rb $\sim 10^2$), the following cycle was adopted: isotope A, ^{95}Rb, 2×180 sweeps (9 s); isotope B, ^{97}Rb, 8×180 sweeps (36 s); isotope C, ^{98}Rb, 17×180 sweeps (76.5 s). The full spectrum was obtained for 10 cycles of this type. One can notice the low background of isotope C obtained owing to the moving dynode. Without it, the background would have been about 400 counts, hiding completely the ^{98}Rb peak.

measures very precisely. In order to determine exactly the values of V that will give coincident trajectories, the ion beam is swept back and forth across slit S_2 by adding to the main dc potential V^0 a small calibrated triangular modulation v. The linearity of v is better than 1%. Each mass peak is then recorded twice with a multiscaler synchronized with the modulation. As seen on Fig. 4 the position of the center of gravity of these peaks gives a measure of the voltage increment v at the time when the ion beam passes the slit. These voltages v are then added to the main voltages V^0 which are measured directly through a

resistor bridge by a digital voltmeter—DVM—
(see Sec. III A)

$$V^0_{A,B} + v_{A,B} = V_{A,B} .$$

In principle, to maintain proportionality between V and U, one should also modulate the accelerating voltages U. In practice this is not done and only V^0 and U are maintained strictly proportional. Not modulating U introduces a systematic bias which is taken into account in the calibration procedure of the modulation.

As was already the case in Ref. 2 possible systematic errors are taken into account by always comparing 3 masses M_A, M_B, M_C, two of which are known from previous measurements so that

$$M_A(V_A + \delta) = M_B(V_B + \delta) = M_C(V_C + \delta) \qquad (1)$$

will determine the "unknown" mass M_C from the potentials V_A, V_B, V_C. δ is a common offset for these three voltages in each measurement.

C. Measurement procedure

For each measurement, the ISOLDE magnetic field is programmed to jump to values corresponding to the 3 masses M_A, M_B, M_C of the isotopes A, B, C under study. Simultaneously the dc potentials U and V^0 are set to the appropriate values. We determine the timing to average the fluctuations with time: On each isotope the 40 Hz modulation of v is applied for $n \times 4.5$ s (n is an integer chosen accordingly to the abundance of the isotope). The corresponding pair of peaks is registered in a given section of the multiscaler memory. Simultaneously the electrostatic potential V^0 is measured repeatedly every two seconds; each measurement lasts one second and the result is directly stored on a PDP 9 computer. Upon completion, a "mass jump" occurs and the next isotope in the sequence is measured. After the jump, before starting again accumulation and voltage measurements, one waits 4.5 s for all power supplies to reach stable values. The sequence of jumps A, B, C, is repeated until adequate statistics are reached. The data are then transferred from the multiscaler to the computer and stored on magnetic tape. They are immediately processed in order to calculate the voltage increment v and a preliminary value of the measured mass. This determination of v allows us to adjust V^0 for the next measurement of the same sequence A, B, C so that the uncertainty in the calibration is negligible in the error estimation.

III. DATA PROCESSING

A. The experimental errors

From Eq. (1) one can see that the experimental error essentially comes from the potential determinations

$$\frac{dM}{M} = \frac{dV}{V} = \frac{dV^0}{V} + \frac{dv}{V} , \qquad (2)$$

$$= \frac{dV^0}{V} + \frac{dv}{\Delta v}\frac{\Delta v}{V} . \qquad (3)$$

dV^0/V is the precision on the dc potential measurement of the electrostatic sector. An accuracy of better than a few times 10^{-7} has been reached by comparing V^0 (divided by a suitable resistor bridge) to a standard 10 volts reference cell, stable to 10^{-7}. The residual potential of about one volt is measured by a six digit digital voltmeter.

The second term of Eq. (2) dv/V is related to the statistics and to the resolution of the mass spectrometer. As seen in (3) it can be separated in two factors: (i) $dv/\Delta v$ is the uncertainty on the position of the center of gravity of the peak relative to its width Δv. To a first approximation

$$\frac{dv}{\Delta v} \propto (N_0 T)^{-1/2} ,$$

where N_0 is the number of ions coming from ISOLDE, and T the transmission of the mass spectrometer

$$(ii) \frac{\Delta v}{V} = \frac{\Delta M}{M} = \frac{1}{R_p} ,$$

where R_p is the resolving power of the mass spectrometer.

The optimal accuracy is thus obtained when $R_p\sqrt{T}$ is maximum, which occurred for $R_p \simeq 5000$ and $T \simeq 10^{-3}$ in our experimental conditions. To this transmission corresponds a value of $dv/\Delta v \simeq 10^{-2}$ to 10^{-3} according to the production yield of ISOLDE (Fig. 2). Taking into account both the accuracy on potential measurements and on the statistics the relative uncertainty on V, i.e., the experimental part of the uncertainty on M, lies between 2×10^{-6} and 2×10^{-7} except for the neutron-deficient rubidium isotopes measured at a time when the precision on the direct measurement of the voltage V^0 by the DVM was only 10^{-6}.

Such a high precision requires a corresponding stabilization of the magnetic and electrostatic fields (better than 10^{-6} over the period of one measurement). However, a stability of the accelerating voltage of a few times 10^{-5} is sufficient due to the energy focusing properties of the mass spectrometer. These stability requirements are not met by the main power supplies of ISOLDE.

This is only one of the many reasons it was found impractical to use ISOLDE as a mass spectrometer and the present arrangement of stopping the ISOLDE beam before the mass spectrometer stage was adopted.

B. The data processing method

As explained above, in one measurement the unknown mass of an isotope X is determined from the known masses of 2 other isotopes α, β, and from the measurement of the voltages applied to the corresponding ions as they follow the same trajectory in the mass spectrometer.

This measurement is normally repeated 5 to 7 times and the mass $M_r(X)$ of the isotope X in terms of the couple (α, β) is determined by the weighted mean

$$M_r(X) = \sum_i m_i M_r^i(X) \Big/ \sum_i m_i \text{ with } m_i = [1/\sigma_\rho^i(X)]^2 .$$

$M_r^i(X)$ is the ith measurement of the mass of X in the sequence $r = X$, α, β. $\sigma_\rho^i(X)$ is the corresponding experimental standard deviation. Other reference couples are chosen, changing one or both of α, and β and $M_s(X)$, $M_t(X)$... are determined.

The final result for the mass $M(X)$ is obtained from

$$M(X) = \sum_r \mu_r M_r(X) ,$$

the μ_r being determined from the minimization of the total error:

$$[\sigma(X)]^2 = [dM(X)]^2$$
$$= \left[\sum_r \mu_r dM_r(X)\right]^2 \quad \text{(see Appendix A)}.$$

The masses of the neutron-deficient as well as of the neutron-rich isotopes of rubidium and cesium have thus been determined step by step: Those of the isotopes near stability are directly deduced from reference masses taken in the 1977 Atomic Mass Table[14]; further out, our own measurements are used as references for the mass determination of increasingly exotic nuclei. An effective limit to our ability to compare directly two masses X and β comes from count rate considerations. It is seen from Fig. 2 that the production yields for different isotopes can vary by as much as 7 orders of magnitude. Taking into account the pileup corrections which we applied, the maximum counting rate which we could accept safely was limited to 10^6/s for the most abundant isotope in a sequence. The propagation of errors through successive measurements and the correlations (due to reference masses) between some of them have been taken into account as explained in Appendix A.

In order to check the validity of the procedure, sequences comprising three known masses were "measured." Care was taken to choose for that purpose isotopes safe from possible isomer or natural isobar contamination. This restricted the available test sequences to relatively few and the results (Table I) show no indication for systematic bias.

IV. RESULTS

The detailed experimental results obtained with the method explained above are presented in Tables II–V and the mass excesses adopted at present in Tables VI and VII. For the rubidium isotopes they represent 10 new masses and 6 masses are better determined than in the 1977

TABLE I. Results of the test sequences. In the deviation $a\sigma$, $a = \dfrac{(M\text{-}A)_{\text{exp}} - (M\text{-}A)_{\text{tab}}}{(\sigma^2_{\text{exp}} + \sigma^2_{\text{tab}})^{1/2}}$

	Sequence	$(M\text{-}A)_{\text{exp}}$ (keV)	$(M\text{-}A)_{\text{tab}}$ (1977 tables, Ref. 14) (keV)	deviation
Fission produced rubidium	83-85-87	$M(83) = -79065 \pm 62$	$M(83) = -78987 \pm 32$	-1.1σ
	87-88-89	$M(87) = -84540 \pm 53$	$M(87) = -84596 \pm\ \ 3$	$+1.0\sigma$
	81-83-85	$M(81) = -75500 \pm 75$	$M(81) = -75445 \pm 35$	-0.7σ
	81-82-83	$M(81) = -75564 \pm 68$	$M(81) = -75445 \pm 35$	-1.6σ
Spallation produced rubidium	80-81-83	$M(80) = -72178 \pm 67$	$M(80) = -72190 \pm 23$	$+0.2\sigma$
Spallation produced cesium	128-131-132	$M(128) = -85966 \pm 150$	$M(128) = -85936 \pm\ \ 6$	-0.2σ
	128-129-131	$M(128) = -85792 \pm\ \ 60$	$M(128) = -85936 \pm\ \ 6$	$+2.4\sigma$

Atomic Mass Table. For the cesium isotopes, 12 are new masses and 6 masses are better determined.

One can notice that the accuracy reached is around 100 keV for isotopes around $A = 100$. This is a significant precision from the physics point of view since the root mean square differences between known and predicted masses stand between 200 and 700 keV.[1] This 100 keV accuracy corresponds to a relative precision on the mass determination of about 10^{-6}. Improvements would be necessary in some cases and are still possible as

TABLE II. Experimental results for the neutron-rich rubidium isotopes.

Measured isotope X	r Sequence	Serial number of the sequence[a]	$(M\text{-}A)_r$ (kev)	Experimental error $\sigma_p(X)$	Total error $\sigma_r(X)$	Statistical weight μ_r	$M\text{-}A$ (keV)	σ (keV)	χ^2 [b]
92	85-89-92	6	−74811	43	49	0.62			0.37
	85-88-92	10	−74889	55	62	0.38			0.60
							−74841	39	
90	85-90-92	7	−79267	24	36	0.24			0.05
	89-90-92	13	−79266	24	30	0.42			0.09
	85-89-90	5	−79292	31	35	0.34			0.24
							−79275	24	
91	85-90-91	8	−77860	30	41	0.5			2.2
	85-91-92	9	−77738	25	41	0.5			2.2
							−77799	34	
93	90-91-93	22	−72736	64	101	0.32			0.03
	91-92-93	23	−72762	46	73	0.68			0.01
							−72754	64	
95	89-93-95	14	−65840	39	104	0.59			0.01
	90-93-95	19	−65823	42	111	0.18			0.07
	91-92-95	24	−65904	97	144	0.23			0.13
							−65852	97	
94	89-92-94	12	−68701	42	76	0.10			0.21
	90-94-95	18	−68731	26	70	0.3			0.002
	90-93-94	20	−68740	34	73	0.13			0.003
	90-92-94	21	−68740	47	67	0.47			0.004
							−68736	44	
96	89-93-96	15	−61253	49	123	0.16			0.06
	89-95-96	16	−61126	38	121	0.24			0.49
	89-94-96	17	−61241	46	74	0.85			0.06
	92-95-96	28	−61209	37	130	−0.25			0.01
							−61223	71	
94[c]	91-94-96	25	−68510	25	51	1	−68510	51	
97	91-94-97	26	−58451	51	101	0.41			0.52
	92-96-97	29	−58382	42	95	0.41			0.01
	93-95-97	30	−58162	50	153	0.18			1.48
							−58370	81	
98	91-94-98	27	−54315	86	135	0.24			0.79
	93-97-98	31	−54185	74	119	0.28			0
	94-96-98	33	−54179	69	133	0.25			0.002
	95-97-98	34	−54069	74	123	0.23			0.97
							−54185	99	
99	93-97-99	32	−50770	148	183	0.72			0.21
	95-98-99	35	−51063	237	262	0.28			0.59
							−50853	164	

[a] The serial numbers of the sequences indicate the order in which the measurements have been done during the experiment. Our aim was to do, as far as possible, the measurements of the same mass through the various sequences at different times.

[b] The apparently high coherence of $\chi^2 = [M_r(X) - M(X)]^2 / [\sigma_r(X)]^2$ comes from the errors on the reference masses which are included in $\sigma_r(x)$.

[c] A mixture of the ground-state and isomeric masses is measured in this sequence (due to an increase of the temperature of the tantalum tube—see text).

TABLE III. Experimental results for the neutron-deficient rubidium isotopes.

Measured isotope X	r Sequence	Serial number of the sequence	$(M-A)_r$ (kev)	Experimental error $\sigma_p(X)$	Total error $\sigma_r(X)$	Statistical weight μ_r	M-A (keV)	σ (keV)	χ^2
82	80-82-83	11	−76080	32	40		−76080	40	
79	79-81-83	6 + 20	−70898	51	90	0.33			
	79-80-81	18	−70844	42	71	0.42			0.46
	79-80-82ᵃ	19	−70964	56	66	0.25			1.19
							−70892	41	
78	78-79-80	13 + 24	−67030	48	85	0.03			0.29
	78-79-82ᵃ	22	−67133	38	69	0.54			0.68
	78-81-82ᵃ	23	−66892	133	220	0.04			0.70
	78-79-81	25	−67022	45	75	0.38			0.52
							−67076	64	
77	77-79-80	4	−64834	78	126	0.47			2.60
	77-78-79	14	−65214	79	121	0.53			2.14
							−65037	105	
76	76-77-79	3	−60745	105	175	0.22			0.19
	76-77-78	28 + 30	−60571	38	164	0.05			0.35
	76-77-79	29	−60652	56	153	0.72			0.01
							−60668	151	
75	75-76-78	26 + 27	−57299	56	207	0.37			0.58
	75-76-77	33	−57327	60	225	−0.16			0.33
	75-77-79	34	−57507	68	189	0.80			0.07
							−57461	188	
74	74-75-76	31	−52097	338	421	0.72			0.05
	74-75-77	32	−51759	555	603	0.28			0.16
							−52002	379	

ᵃThe mass excess of ^{82}Rb used here is the one determined by sequence 11 (mixture of ground state and isomer mass); see Appendix B.

will be discussed later.

The case of $^{74}_{37}$Rb$_{37}$ is especially interesting. A precision of $\simeq$100 keV on its mass (together with a reasonably accurate half-life[15]) would lead to a meaningful determination of the $\mathcal{F}t$ value for the superallowed transition

$$^{74}\text{Rb} \xrightarrow{\beta^+} {}^{74}\text{Kr}.$$
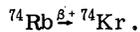
The importance of these $\mathcal{F}t$ determinations in connection with the fundamental theories of weak interactions and the mass of the intermediate boson was shown by Towner *et al.*[16] and Wilkinson.[17] As discussed elsewhere[12] it appears possible in the near future to measure the mass of ^{74}Rb to that level of accuracy.

We would like to stress further two important points:

(i) Each of our mass measurements depends on the reference masses (quoted in Tables VI and VII) and on the previously measured masses (the order of processing is the one presented in each of Tables II–V). Should one of the references change it would be easy (see Appendix A) to deduce the correction that must be applied to the relevant masses.

Some of the masses which were selected as references for their relatively good accuracy in the 1977 Atomic Mass Table appear to be "secondary data"[14] from Q_β measurements and would have to be confirmed by direct mass measurements. This is especially the case for the isotopes ^{81}Rb, ^{83}Rb, ^{127}Cs, ^{129}Cs, ^{139}Cs. The masses of isotopes near stability should be known as precisely as possible as they serve as references for the measurements of masses further away from stability. Furthermore, it was realized in the course of the experiment that each mass had to be measured through several different sequences; this explains why some have been measured in two sequences only and others in much more. This lack of balance could be improved in the future.

(ii) Isomers cannot be separated from the ground state with the present method. To separate an excited level of 100 keV above the ground state (g.s.) for $A = 100$ would require a resolving power of 10^6. Consequently if some isomers are produced together with the ground state in the fission or spallation reactions, the values given in Tables

TABLE IV. Experimental results for the neutron-rich cesium isotopes.

Measured isotope X	r Sequence	Serial number of the sequence	$(M-A)_r$ (kev)	Experimental error $\sigma_\rho(X)$	Total error $\sigma_r(X)$	Statistical weight μ_r	M-A (keV)	σ (keV)	χ^2
140	131-139-140	4	-76962	46	92	0.51			0.05
	132-139-140	10	-77005	44	92	0.49			0.06
							-76983	86	
142	132-140-142	7	-70405	49	120	0.41			0.02
	132-139-142	8	-70435	53	116	0.58			0.01
	139-140-142	13	-70334	114	180	0.01			0.23
							-70421	110	
138	137-138-139	30	-82845	35	50	0.41			0.18
	137-138-142	31	-82881	38	44	0.59			0.12
							-82866	38	
141	131-139-141	5	-74493	53	104	0.24			1.24
	132-139-141	9	-74347	51	105	0.18			0.08
	139-141-142	14	-74276	41	114	0.01			0.78
	140-141-142	20	-74371	36	103	-0.03			0.003
	137-141-142	29	-74322	41	96	0.48			0.33
	131-140-141	6	-74487	47	107	0.11			1.06
							-74377	91	
144	139-142-144	12	-63151	74	161	0.89			0.002
	141-142-144	23	-63220	116	208	0.11			0.09
							-63159	161	
143	139-141-143	15	-67489	86	148	0.40			0.43
	140-143-144	22	-67604	51	147	0.19			0.01
	142-143-144	26	-67673	46	140	0.41			0.39
							-67586	130	
145	139-142-145	11	-60119	95	187	0.45			0.32
	139-144-145	16	-59976	65	194	0.25			0.04
	140-143-145	21	-59800	130	215	0.17			0.98
	141-143-145	24	-59983	88	203	0.15			0.02
	143-144-145	27	-59881	89	231	-0.02			0.33
							-60013	172	
146	140-145-146	19	-55700	90	195	0.89			0.11
	143-144-146	28	-55092	149	313	0.11			3.0
							-55634	193	
147	140-145-147	18	-52557	236	320	0.83			0.33
	141-144-147	25	-51491	496	558	0.17			2.50
							-52373	305	

II–V include their possible contribution. Indeed if $M_{g.s.}(X)$ is the ground-state mass of the isotope X and $M(X)$ the measured mass of this isotope (including the ground-state mass and the mass of the isomer with excitation energy Δ)

$$M_{g.s.}(X) = M(X) - \frac{R}{R+1}\Delta .$$

R is the population ratio of the isomer ^mA relative to the ground state A in the ISOLDE beam. It can be determined by other experiments at ISOLDE,[18] so that if Δ is known, $M(X)$ can be corrected to give the true value of the ground-state mass. Corrections could thus be made for ^{78}Rb and ^{90}Rb.

Moreover, it has to be pointed out that if a measured mass is not a pure ground-state mass but a mixture including an isomeric contribution, the masses measured from it, in the same experiment are still correct (see for example Table III where the ^{82}Rb mass used is not the true ground-state mass but the measured mixture and Appendix B).

The above assumes that the delays introduced by the desorption of ISOLDE ions from our tantalum tube do not alter R as is generally the case. This will no longer be true if the delay is such as to cause different losses to the isotope A and to its isomer ^mA. We found a case where, due to particular combination of half-lives and delay time, the ratio R varies appreciably with the temperature of the tantalum tube. Following an increase of this temperature the value measured for the mass of ^{94}Rb varied during the course of the run. Even
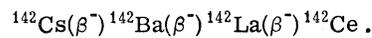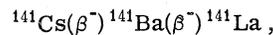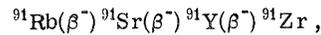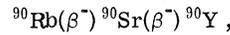
though the four sequences 12, 18, 20, 21 (Table II) give for this isotope a mean value of mass excess $M-A = -68736 \pm 44$ keV, after the sequence 24 (corresponding to the increase of the temperature) all the sequences (25, 26, 27, 33) using ^{94}Rb give inconsistent results if one assumes this value for its mass excess. They give consistent results, however, with a value about 200 keV less bound. This seems to indicate the existence of a new isomer ^{94m}Rb. Its intensity increases (relative to the g.s.)with the temperature, therefore its half-life should be shorter than that of the g.s. ($T = 2.7$ s). Its excitation energy should be

$$\Delta > (220 \pm 70) \text{ keV} .$$

In the sequences 26, 27, 33, the value $M-A = -68510 \pm 50$ keV was assumed for ^{94}Rb + ^{94m}Rb as obtained from the sequence 25 (91-94-96).

A. Comparison with the mass values of the 1977 Atomic Mass table[14]

As can be observed in Tables VI and VII, discrepancies occur for some neutron-rich rubidium and cesium isotopes. We point out that the Mass Table values for these isotopes are not direct mass measurements but masses deduced from "primary nuclides"[14] through Q_β measurements in the following chains

$$^{90}\text{Rb}(\beta^-)\,^{90}\text{Sr}(\beta^-)\,^{90}\text{Y} ,$$

$$^{91}\text{Rb}(\beta^-)\,^{91}\text{Sr}(\beta^-)\,^{91}\text{Y}(\beta^-)\,^{91}\text{Zr} ,$$

$$^{141}\text{Cs}(\beta^-)\,^{141}\text{Ba}(\beta^-)\,^{141}\text{La} ,$$

$$^{142}\text{Cs}(\beta^-)\,^{142}\text{Ba}(\beta^-)\,^{142}\text{La}(\beta^-)\,^{142}\text{Ce} .$$

If some of the level schemes of these isotopes

TABLE V. Experimental results for the neutron-deficient cesium isotopes.

Measured isotope X	r sequence	Serial number of the sequence	$(M\text{-}A)_r$ (keV)	Experimental error $\sigma_\rho(X)$	Total error $\sigma_r(X)$	Statistical weight μ_r	$M\text{-}A$ (keV)	σ (keV)	χ^2
126	126-127-128	29	−84175	62	75	0.30			0.85
	126-128-129	30	−84272	94	106	0.14			0.07
	126-128-131	31	−84273	52	53	0.57			0.30
							−84244	40	
124	124-126-128	4 + 26	−81404	61	100	0.35			0.88
	124-125-128	27	−81530	42	67	0.48			0.23
	124-125-126	28	−81598	61	108	0.17			0.86
							−81498	54	
123	123-126-128	23	−80754	77	125	0.25			0.01
	123-124-128	24	−80789	55	86	0.35			0.09
	123-124-126	25	−80745	49	90	0.40			0.04
							−80763	72	
122	122-124-126	18	−77710	60	115	0.24			0.01
	122-124-128	21	−77681	46	92	0.54			0.03
	122-126-128	22	−77727	99	153	0.22			0.04
							−77698	84	
121	121-123-126	16	−76638	50	118	0.72			0.03
	121-124-126	17	−76710	75	143	0.28			0.13
							−76658	113	
120	120-121-124	12	−73297	45	143	0.85			0.01
	120-123-124	14	−73210	123	209	0.15			0.13
							−73284	140	
119	119-120-121	9	−71535	59	186	0.04			0.10
	119-120-124	11	−71605	39	169	1.13			0.003
	119-120-122	34	−71645	79	200	−0.18			0.06
							−71595	168	
118	118-119-120	6	−67511	68	215	0.42			0
	118-119-121	7	−67512	50	208	0.57			0
	118-120-121	8	−67521	93	237	0.01			0.001
							−67512	199	
117	117-118-119	2	−65228	102	248	0.65			0.13
	117-118-120	3	−65379	184	308	0.09			0.04
	117-119-120	5	−65516	138	281	0.27			0.50
							−65318	239	

TABLE VI. Mass excesses of the rubidium isotopes.

A	$(M\text{-}A)$ adopted values (keV)	$(M\text{-}A)$ (1977 Atomic Mass Table, Ref. 14) (keV)	Deviation[g]	
74	-52000 ± 380			
75	-57460 ± 190	-57510 ± 600[b]	(0.08σ)	
76	-60670 ± 150[a]	-60610 ± 270[b]	(0.2σ)	
77	-65040 ± 110[a]	-65110 ± 120[c]	(0.5σ)	
78	-67145 ± 65[d]	-67090 ± 180[b]	(0.3σ)	
79	-70892 ± 40[a]	-70860 ± 110	0.3σ	
80		-72190 ± 23[e]		
81		-75445 ± 35[e]		
82		-76213 ± 20[e]		
83		-78987 ± 32[e]		
84		-79752 ± 4		
85		-82159 ± 4[e]		
86		-81738 ± 3		
87		-84596 ± 3		
88		-82602 ± 12[e]		
89		-81717 ± 13[e]		
90	-79346 ± 24[f]	-79570 ± 60	3.5σ	
91	-77800 ± 35[a]	-77970 ± 40	3.3σ	
92	-74840 ± 40[a]	-75120 ± 200	1.4σ	
93	-72755 ± 65	-72920 ± 170	0.9σ	
94	-68735 ± 45	-69460 SYST		$+725$ keV
95	-65850 ± 100	-66550 ± 310	2.1σ	
96	-61220 ± 70	-62770 SYST		$+1550$ keV
97	-58370 ± 80			
98	-54180 ± 100			
99	-50850 ± 160			

[a] No isomers have been observed at ISOLDE in the ABMR experiments (Ref. 18).

[b] These values are our own preliminary results communicated to A. H. Wapstra with increased errors. Their deviations are therefore within parentheses.

[c] Value from 1975 table (-65240 ± 150) combined with our preliminary result (-64920 ± 120).

[d] The experimental measurement has been corrected for an isomer ($R = 2 \pm 0.5$, $\Delta = 103$ keV).

[e] Adopted values for the primary reference masses. The precisely known masses of stable isotopes or of isotopes with isomeric state have not been used (except for ^{82}Rb which isomer has been taken into account, see Appendix B).

[f] The experimental measurement has been corrected for an isomer ($R = 2 \pm 1$, $\Delta = 107$ keV).

[g] The deviation is quoted in keV when the Atomic Mass Table (Ref. 14) value is an extra or intrapolation value (precision quoted SYST in Ref. 14). $a\sigma$ has the same meaning as in Table I.

are not well established the Q_β are lower limits giving rise to higher binding energies. Our measurements always indicate lower bindings than the table values. This could also be due to an isomeric contribution. Nevertheless the correction for isomer contribution has already been applied for ^{90}Rb (see Table VI) and a 200 keV discrepancy still remains. For the other cases no isomers have been observed at ISOLDE.

V. DISCUSSION

The measured and the predicted[1] masses will be compared and the origin of discrepancies for isotopes far from stability briefly discussed.

Moreover, from the long series of neutron separation energies (data from $N = 37$ to 62 for $Z = 37$, and from $N = 62$ to 92 for $Z = 55$) that are available for the first time as a result of this work, one can deduce direct model independent information. We draw attention to some nuclear structure features (sudden changes in nuclear shapes, pairing energies, shell closures) that seem to emerge from these data.

A. Comparison with the mass predictions

The measured mass excesses are compared in Figs. 5(a), 5(b), 5(c), and 5(d) with the values presented in the 1975 Mass Predictions,[1] which

are the results of nine different mass formulas
fitted to either the 1971 Atomic Mass Evaluation[19]
or the 1975 Midstream Atomic Mass Evaluation.[20]

All these mass formulas do not extend their
predictions far from stability with the same ac-
curacy. The semiempirical shell model predic-
tions[21] stay within 1 to 1.5 MeV from the experi-
mental values for both rubidium and cesium iso-
topes [see Figs. 5(c) and 5(d)]. The masses cal-
culated according to the mass relations of the
Garvey-Kelson type[22-24] are of the same order of
accuracy for the rubidium isotopes but deviate up
to 2 to 3 MeV for the cesium isotopes. However,
this corresponds to the accuracy quoted by Comay
and Kelson[23] for such long extrapolations.

Regarding the three different liquid drop calcula-
tions[25-27] we consider their results according to

each element cesium and rubidium [see Figs. 5(a)
and 5(b)].

(i) For the cesium isotopes their predictions far
from stability are comparable between each other
and to those given by the Mass Relations. A com-
pletely different and particularly good fit is ob-
tained with the old drop model[28] of Myers and
Swiatecki (1966).

(ii) For the rubidium isotopes the three liquid drop
calculations do not have the same behavior. Seeger
and Howard[25] obtain masses with an accuracy of
1 to 2 MeV, whereas the masses calculated by
Groote *et al*.[27] and Myers[26] deviate regularly from
the experimental ones up to 5 MeV on the neutron-
rich side. Toward the neutron-deficient rubidium
isotopes one can observe the influence of the so-
called Wigner term when comparing the curves

TABLE VII. Mass excesses of the cesium isotopes.

A	(M-A) adopted values (keV)	(M-A)$_{tab}$ (1977 tables, Ref. 14) (keV)	Deviation	
117	-65320 ± 240	-66850 SYST		+ 1530 keV
118	-67510 ± 200^a	-68670 SYST		+ 1160 keV
119	-71600 ± 170^b	-72530 SYST		+ 930 keV
120	-73280 ± 140^a	-73640 ± 320	1.0σ	
121	-76660 ± 110^b	-77150 SYST		+ 490 keV
122	-77700 ± 85^b	-78010 SYST		+ 310 keV
123	-80760 ± 70	-80890 SYST		+ 130 keV
124	-81500 ± 55	-81530 ± 480	0.1σ	
125		-84040 ± 40		
126	-84244 ± 40	-84330 ± 140	0.6σ	
127		-86206 ± 21^c		
128		-85935 ± 6^c		
129		-87563 ± 24^c		
130		-86863 ± 12		
131		-88066 ± 8^c		
132		-87175 ± 23^c		
133		-88089 ± 8		
134		-86909 ± 8		
135		-87665 ± 9		
136		-86358 ± 8		
137		-86560 ± 7^c		
138	-82870 ± 40^b	-82770 SYST		- 100 keV
139		-80630 ± 70^c		
140	-76980 ± 90^d	-77240 ± 250	1.0σ	
141	-74380 ± 90^d	-75000 ± 100	4.6σ	
142	-70420 ± 110^d	-70950 ± 130	3.1σ	
143	-67590 ± 130^d	-68360 SYST		+ 770 keV
144	-63160 ± 160^d	-63930 SYST		+ 770 keV
145	-60010 ± 170	-61720 SYST		+ 1710 keV
146	-55630 ± 190			
147	-52370 ± 310			

[a] Evidence has been found for an isomeric state (Ref. 49)—no correction has been applied.
[b] Isomer observed (Ref. 48)—the level is not known and no correction has been applied.
[c] Adopted values for the primary reference masses—as for rubidium isotopes.
[d] No isomer has been observed at ISOLDE in the ABMR experiments (Ref. 18).
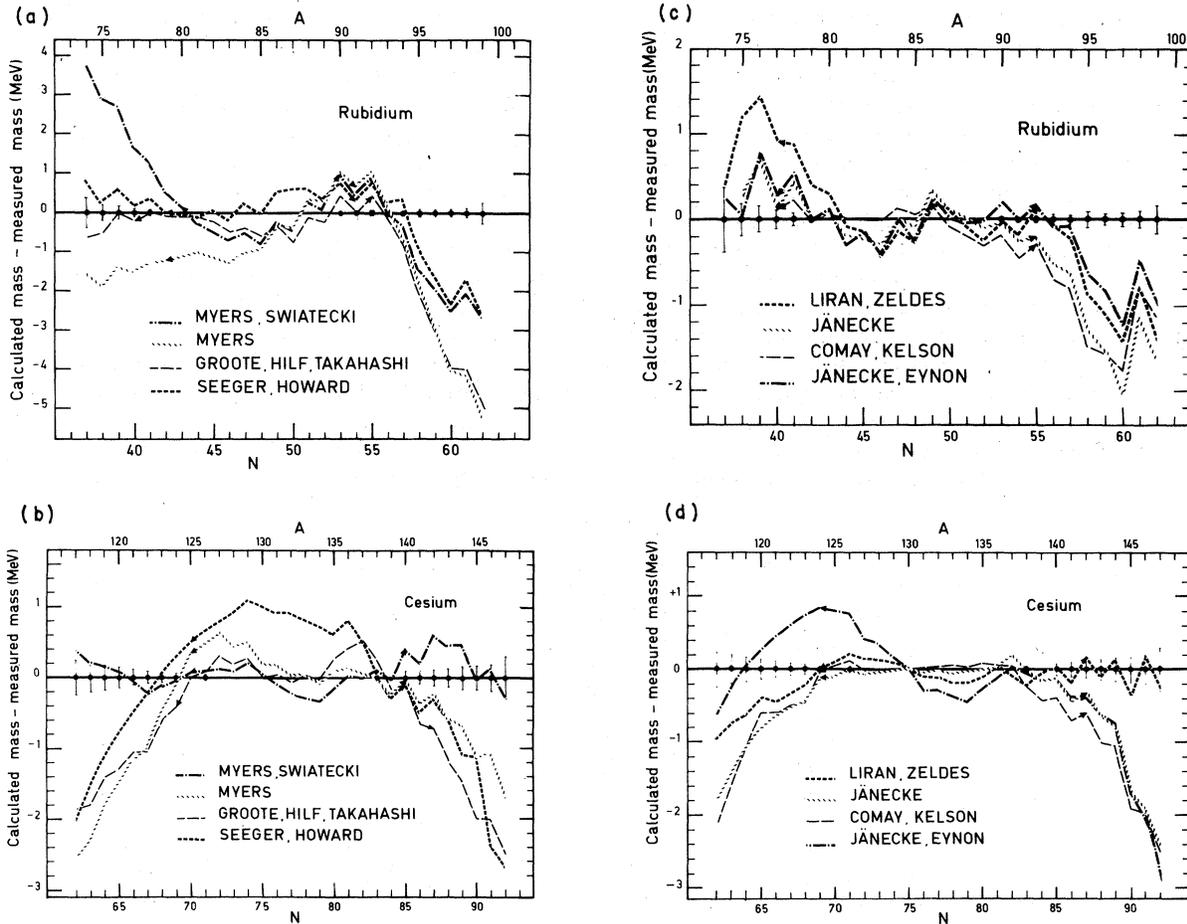
FIG. 5. Difference between calculated and measured mass excesses (a) and (c) for the rubidium isotopes (note the different scales) (b) and (d) for the cesium isotopes. Solid points are the reported measurements with their errors. The arrows indicate the limits of the known masses which were used to fit the predictions.

corresponding to the calculations of Myers and Swiatecki[28] (1966) to those of Myers[26] (1975) [Fig. 5(a)]. Our measurements include ^{74}Rb which is the heaviest known nucleus with $N=Z$ and we thereby extend the study of the influence of this "symmetry term" in the binding energy. In the first liquid drop mass formula of Myers and Swiatecki[28] (1966) the symmetry energy was taken into account only through terms in $(|N-Z|/A)^2 = I^2$. Systematic $|I|$ dependent deviations observed at the time suggested the introduction of a short range corrective term (i.e., $\exp[-k\,|I|]$). Our results also support such a correction. Nevertheless, all recent liquid drop calculations[25-27] use instead a term linear in $|I|$ for which there seems to be a better physics justification.[26] It improves the fit for the small values of $|I|$ near $N=Z$, but it is not clear whether it is the best choice if one considers high values of $|I|$.

Considering the droplet model calculations an attempt was made to analyze the different components of the shell corrections added to the droplet term (which in fact include the shape dependent part of the droplet itself). As shown in Fig. 6 the spherical shell part alone in the calculations of Myers[26] (as well as in those of Groote et al.[27]) seems to be in better agreement with the experimental shell than the total shell corrections. The arches on either side of the magic shells ($N=50$ and $N=82$) flatten too much, suggesting that the deformation starts further than predicted.

B. The one-neutron and two-neutron separation energies

The one-neutron separation energies S_n deduced from our mass measurements have been plotted for the rubidium and cesium isotopes (e.g. Fig. 7). From these plots one can calculate the neu-
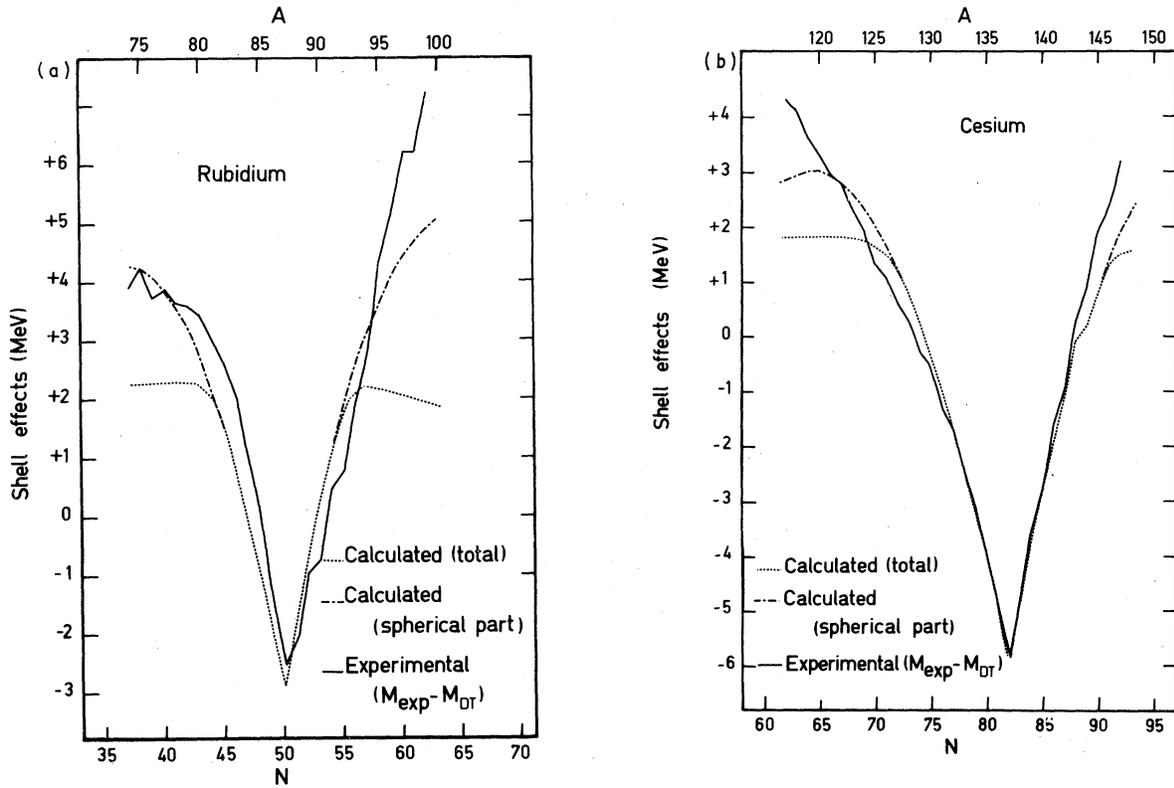
FIG. 6. Comparison between experimental and calculated (total and spherical part) shell terms of the droplet model of Myers (Ref. 26). The experimental shell effect is obtained as usual by subtracting the droplet terms M_{DT} from the experimental mass. (a) Rubidium isotopes, (b) cesium isotopes.
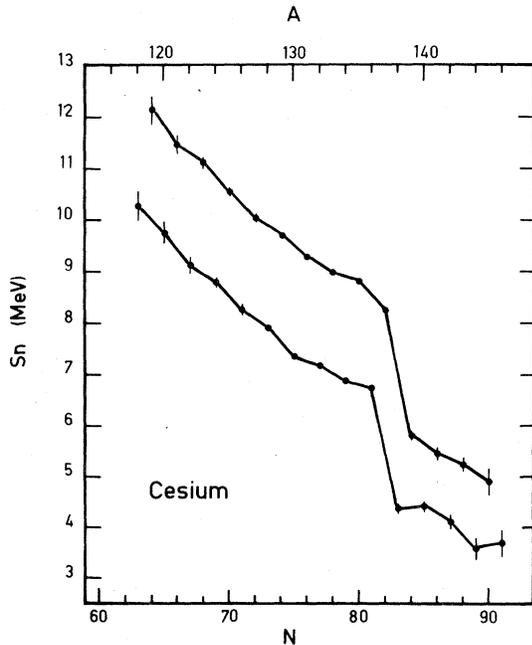

FIG. 7. Experimental one-neutron separation energies S_n of the cesium isotopes. The upper curve joins even N points and the lower one joins odd N points.

tron pairing energy which is related to the distance between the even N and odd N curves, and is given by[29]

$$\Delta_n = \frac{(-1)^N}{4}[2S_n(N,Z) - S_n(N+1,Z) - S_n(N-1,Z)].$$

As already observed, Fig. 7 shows that Δ_n is much weaker after the shell closure than before. Mean values $\overline{\Delta}_n$ have been deduced from the smooth parts of the curves, away from shell or subshell closures and other nuclear structure effects. They are reported in Table VIII and compared with the pairing terms from liquid drop mass formulas which are in general independent of shell structure. They have then been used to avoid the systematic odd-even variation associated with S_n: Figure 8 shows the variation of $S_n \pm \overline{\Delta}_n$ as a function of N. The two-neutron separation energies S_{2n} have also been plotted for the rubidium and cesium isotopes, as well as for the neighboring elements (Fig. 9) and the same kind of observations can be drawn from their behavior.

On the rubidium S_n and S_{2n} curves, after the well known discontinuity corresponding to the $N = 50$ closed shell, a break of the slope appears

TABLE VIII. Experimental and theoretical neutron pairing energies in keV. Experimental values are the mean of the quantity $[(-1)^N/4]$ $[2S_n^N - S_n^{N+1} - S_n^{N-1}]$ for the smooth parts of the S_n curve. It represents in fact the difference between the neutron-neutron and neutron-proton pairing energies $\Delta nn - \Delta np$ to take into account the extra binding energies of the odd-odd nuclei (Ref. 30). The theoretical values are calculated respectively for $A = 81, 94, 128,$ and 142.

| | Rubidium $Z = 37$ | | Cesium $Z = 55$ | |
	$N < 50$	$N > 50$	$N < 82$	$N > 82$
Experimental	1113 ± 20	570 ± 17	1008 ± 6	630 ± 20
Myers and Swiatecki, Ref. 28	1222	1135	972	923
Myers, Ref. 26	1086	1025	904	866
Groote, Hilf and Takahashi, Ref. 27	1111	1031	884	839
Seeger and Howard, Ref. 25	1250	1000	1050	880

between $N = 56$ and $N = 57$ and can be correlated to the closure for spherical nuclei of the neutron subshell $d5/2$ enhanced near $Z = 38$ by the closure of the proton subshell $f5/2$. Then a hump occurs at $N = 60$ which is reminiscent of the one observed in the rare earth[31] and in the neutron-rich sodium isotopes[2] and which is associated with a sudden change of the nuclear shape. This was already indicated in this region (centered approximately around ^{102}Zr and extending up to molybden) by the excited states systematics[32-34] and some other experimental facts.[35-40] Many theoretical predictions on this new region of deformation have been carried out since 1969.[41-45] The hump which is

observed here could correspond to the low Z part of this region of deformed nuclei. Another "deformed region" is expected from theoretical calculations such as those of Sheline, Ragnarsson, and Nilsson[46,47] on the neutron-deficient side, and the contour plot of the experimental energy of the first 2+ state (E_{2+}) as a function of N and Z suggests deep minima also around ^{80}Zr. No hump is observed on the neutron-deficient side of the S_{2n} curve of rubidium. The break in the slope under $N = 42$ can be explained either by this deformation or an extra binding energy due to the enhanced p-n interaction when approaching $N = Z$ as suggested by the ^{76}Rb and ^{78}Rb points on the S_n curve [Fig. 8(a)]. The fact that the deformation does not show up as clearly on the neutron-deficient as on
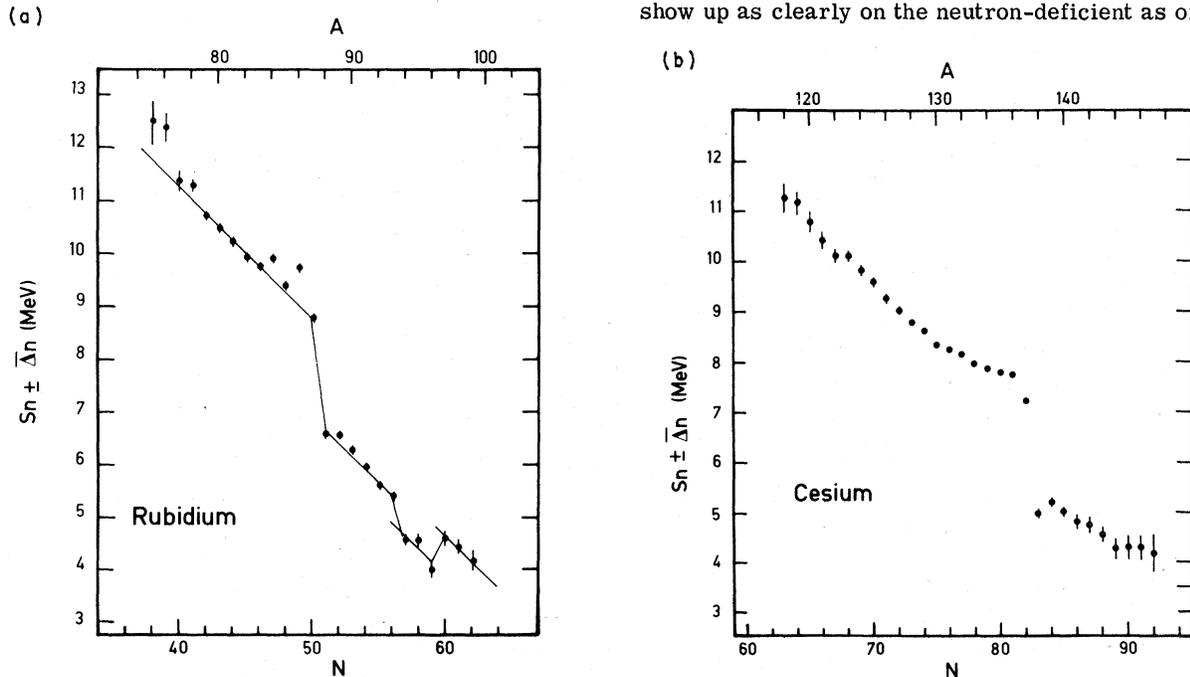

FIG. 8. One-neutron separation energies S_n corrected with the mean neutron pairing energy $\bar{\Delta}_n$ calculated from the smooth part of the curve S_n. (a) Rubidium isotopes, (b) cesium isotopes.
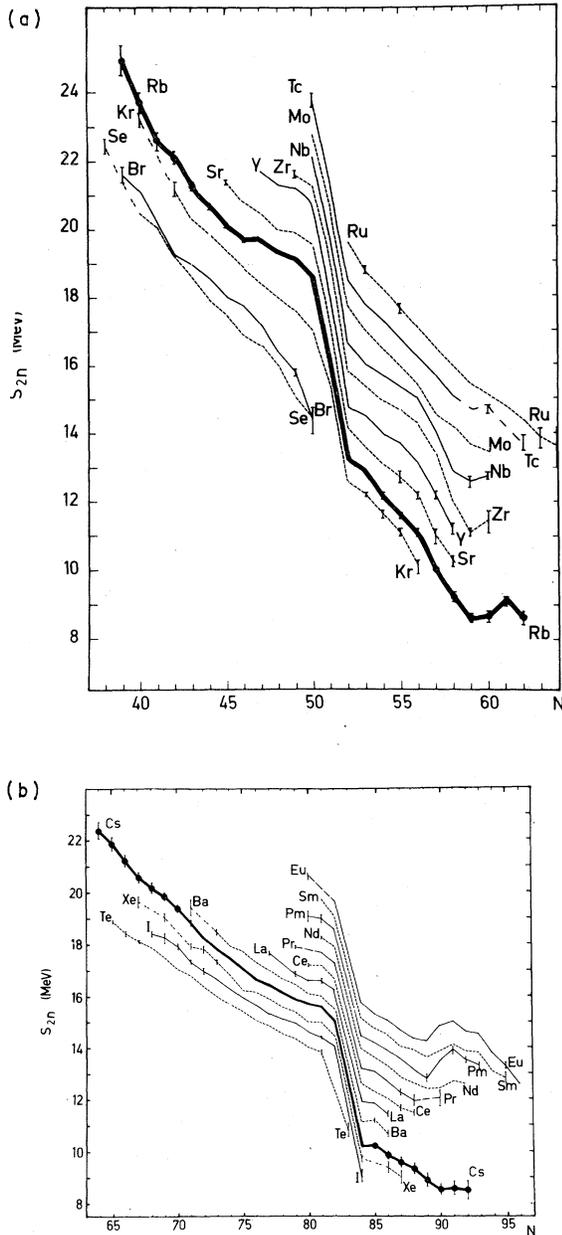
FIG. 9. Experimental two-neutron separation energies S_{2n} versus the neutron number N (a) in the rubidium region, (b) in the cesium region, from the reported mass measurements and from the 1977 Atomic Mass Table (Ref. 14) (excluding systematics extrapolation).

the neutron-rich side may be due to a more progressive change in nuclear shape. This argument is supported by the slower decrease of E_{2+} when N decreases starting from $N = 50$ compared with similar variation of E_{2+} when N increases starting at the $N = 56$ subshell. The same argument could

apply for the neutron-deficient cesium isotopes for which no deformation appears on the S_n or S_{2n} curve; only a break in the slope is observed between $N = 67$ and $N = 69$. On the neutron-rich side of the cesium curve the data suggest that a deformation could set in at $N = 91$. However, because of the large error bars no conclusion can be drawn as of now, on the extension down to $Z = 55$ of the well known deformation of the rare earth region ($N \geqslant 90$).

VI. CONCLUSIONS

We have shown in this work that interesting effects in nuclear structure show up when the masses of an extensive series of isotopes are measured to an adequate degree of accuracy. If necessary (as pointed out in Sec. IV) the precision could still be improved for isotopes either very close to or very far from stability. It would be of obvious interest to extend these measurements to isotope series of other elements. Masses of francium isotopes ($^{204-210,212}$Fr $^{224-228}$Fr) have already been measured and work on other elements is in preparation.

APPENDIX A: EVALUATION OF THE PROPAGATION OF ERRORS ON MEASURED MASSES

1. Reference masses are taken from the Atomic Mass Table

In order to establish how to calculate the final weighted mean value of a mass which has been measured in different sequences, let us first examine the special case where all reference masses are given by the Atomic Mass Table.[14]

The unknown mass $M_r(X)$ is measured in a sequence $r = X, \alpha, \beta$ where α and β are the two references. Their masses $M(\alpha)$ and $M(\beta)$ are taken with the uncertainties $\sigma(\alpha)$ and $\sigma(\beta)$ as quoted in the Atomic Mass Table.[14]

From the basic relation

$$M_r(X)(V_X + \delta) = M(\alpha)(V_\alpha + \delta) = M(\beta)(V_\beta + \delta)$$

we obtain

$$M_r(X) = \frac{M(\alpha)M(\beta)(V_\alpha - V_\beta)}{V_X[M(\beta) - M(\alpha)] + M(\alpha)V_\alpha - M(\beta)V_\beta} \ . \tag{A1}$$

$V_\alpha \ V_\beta \ V_X$ are the corresponding voltages measured as explained in the text. The error on this measurement is calculated from

$$dM_r(X) = \frac{\partial M_r(X)}{\partial V_X}dV_X + \frac{\partial M_r(X)}{\partial V_\alpha}dV_\alpha + \frac{\partial M_r(X)}{\partial V_\beta}dV_\beta$$
$$+ \frac{\partial M_r(X)}{\partial M(\alpha)}dM(\alpha) + \frac{\partial M_r(X)}{\partial M(\beta)}dM(\beta) \ .$$

The first three terms concern the experimental uncertainty for that measurement: σ_p^i (see Sec. III A). The two last terms represent the contribution of the reference mass errors:

$$\frac{\partial M_r(X)}{\partial M(\alpha)}\sigma(\alpha) = \frac{M_r(X)}{M(\alpha)} \frac{M_r(X) - M(\beta)}{M(\alpha) - M(\beta)}\sigma(\alpha)$$
$$\simeq \frac{X}{\alpha}\frac{X - \beta}{\alpha - \beta}\sigma(\alpha) \ ,$$

$$\frac{\partial M_r(X)}{\partial M(\beta)}\sigma(\beta) = \frac{M_r(X)}{M(\beta)} \frac{M_r(X) - M(\alpha)}{M(\beta) - M(\alpha)}\sigma(\beta)$$
$$\simeq \frac{X}{\beta}\frac{X - \alpha}{\beta - \alpha}\sigma(\beta); \tag{A2}$$

X, α, β are the mass numbers of each isotope. This mass measurement of X using the sequence r is repeated n times and the mass of X measured from the couple (α, β) is the mean value of these n measurements weighted with the only experimental errors (the reference masses stay the same)

$$M_r(X) = \frac{\sum\limits_{i=1}^{i=n} M_r^i(X)/[\sigma_p^i(X)]^2}{\sum\limits_{i=1}^{i=n} 1/[\sigma_p^i(X)]^2} \ ; \tag{A3}$$

the experimental part of the error is

$$\sigma_p(X) = \left\{ \sum_{i=1}^{i=n} 1 / [\sigma_p^i(X)]^2 \right\}^{-1/2} \tag{A4}$$

while the total error on $M_r(X)$ is

$$\sigma_r(X) = \left\{ [\sigma_p(X)]^2 + \left[\frac{\partial M_r(X)}{\partial M(\alpha)}\right]^2 \sigma^2(\alpha) \right.$$
$$\left. + \left[\frac{\partial M_r(X)}{\partial M(\beta)}\right]^2 \sigma^2(\beta) \right\}^{1/2} \tag{A5}$$

which includes the contribution of the reference masses as evaluated in Eq. (A2). When varying the references α, β, the ultimate value of the mass $M(X)$ is obtained as

$$M(X) = \sum_{r=1}^{r=m} \mu_r M_r(X) \ , \tag{A6}$$

where m is the total number of sequences. From (A6) we get

$$dM(X) = \sum_r \mu_r dM_r(X)$$

and

$$\sigma^2(X) = \left\{ \sum_r \mu_r \left[\sigma_p(X) + \sum_\alpha \frac{\partial M_r(X)}{\partial M(\alpha)}\sigma(\alpha) \right] \right\}^2 \tag{A7}$$

where, the different σ being independent, all crossed terms such as $\sigma(\alpha)\ \sigma(\beta)$ or $\sigma_p(X)\sigma(\alpha)$ are zero, i.e.,

$$\sigma^2(X) = \sum_r [\mu_r \sigma_p(X)]^2$$
$$+ \sum_\alpha \left[\sum_r \mu_r \frac{\partial M_r(X)}{\partial M(\alpha)} \right]^2 \sigma^2(\alpha) \ . \tag{A8}$$

The weights μ_r are determined by minimizing $\sigma(X)$ with the condition $\sum_r \mu_r = 1$. The Lagrangian multiplier method leads to the resolution of a system with $m + 1$ linear equations and $m + 1$ unknown quantities: $\mu_1, \ \mu_2 \cdots \mu_m, \ \lambda$. λ is the Lagrangian multiplier

$$\sigma_r \sum_{j=1}^{j=m} \sigma_j \mu_j - \lambda = 0 \quad \text{for } r = 1, m$$

and

$$\sum_{j=1}^{m} \mu_j - 1 = 0 \ , \tag{A9}$$

where σ_r is as calculated by Eq. (A5) and

$$\sigma_r \sigma_s = \sum_\alpha \frac{\partial M_r(X)}{\partial M(\alpha)} \frac{\partial M_s(X)}{\partial M(\alpha)}\sigma^2(\alpha)$$

is different from zero only if the two sequences r and s have a common reference mass.

2. Reference masses include preceding measured masses

When measuring further masses, one can include as a secondary reference a mass which has been previously measured. The measured masses, however, still depend on the original Mass Table references. As an example, let us assume that $M(Y)$ is measured in the sequence $p = Y, X, \alpha$. As before, $M_p(Y)$, $\sigma_r(Y)$, $\sigma_p(Y)$, $M(Y)$, $\sigma(Y)$ are obtained by using Eqs. (A3), (A4), (A5), (A6), (A7). However, in order to minimize $\sigma(Y)$, one has now to take into account the fact that $\sigma(X)$ is not independent from $\sigma(\alpha)$, $\sigma(\beta)$.... This is done by using Eq. (7) to express $\sigma(X)$ so that one finally obtains $\sigma(Y)$ as a function of $\sigma_\pi(Y)$, $\sigma_p(X)$, $\sigma(\alpha)$, $\sigma(\beta)$... :

TABLE IX. Neutron-deficient rubidium isotopes data analysis according to the possible assumptions regarding ^{82}Rb.

Measured isotope X	Assumption 1: $M\text{-}A = -76213 \pm 20$ keV (1977 Atomic Mass Table value)				Measured isotope X	Assumption 2: $M\text{-}A = -76080 \pm 40$ keV (from sequence 80-82-83)				Measured isotope X	Assumption 3: $M\text{-}A$ of ^{82}Rb is supposed to be unknown.			
	r seq	$(M\text{-}A)_r$	μ_r	χ^2		r seq	$(M\text{-}A)_r$	μ_r	χ^2		r seq	$(M\text{-}A)_r$	μ_r	χ^2
79	6 + 20	−70898 ± 90	0.33	0.06	79	6 + 20	−70898 ± 90	0.33	0	79	6 + 20	−70898 ± 90	0.41	0.13
	18	−70844 ± 71	0.43	0.20		18	−70844 ± 71	0.42	0.46		18	−70844 ± 71	0.59	0.10
	19^a	−70900 ± 66	0.24	0.13		19^a	−70964 ± 66	0.25	1.19		mean	−70866 ± 45		
	mean	−70876 ± 41				mean	−70892 ± 41							
78	13 + 24	−66998 ± 83	0.06	0	78	13 + 24	−67030 ± 85	0.03	0.29	78	13 + 24	−66978 ± 90	0.32	0
	22^a	−67070 ± 67	0.52	1.06		22^a	−67133 ± 69	0.54	0.68		25	−66984 ± 79	0.68	0
	23^a	−66512 ± 198	0.07	6.10		23^a	−66892 ± 220	0.04	0.70		mean	−66982 ± 75		
	25	−66999 ± 75	0.34	0		25	−67022 ± 75	0.38	0.52					
	mean	−67001 ± 62				mean	−67076 ± 64							
77	4	−64788 ± 124	0.46	1.66	77	4	−64834 ± 126	0.47	2.60	77	4	−64758 ± 133	0.53	0.96
	14	−65082 ± 118	0.54	1.29		14	−65214 ± 121	0.53	2.14		14	−65037 ± 138	0.47	1.17
	mean	−64948 ± 102				mean	−65037 ± 105				mean	−64888 ± 117		
76	3	−60621 ± 170	0.22	0.19	76	3	−60745 ± 175	0.22	0.19	76	3	−60537 ± 209	0.31	0.03
	28 + 30	−60469 ± 161	0.02	0.23		28 + 30	−60571 ± 164	0.05	0.35		28 + 30	−60369 ± 213	−0.38	0.38
	29	−60528 ± 148	0.76	0.02		29	−60652 ± 153	0.72	0.01		29	−60444 ± 189	1.07	0.09
	mean	−60547 ± 145				mean	−60668 ± 151				mean	−60501 ± 185		
75	26 + 27	−57157 ± 202	0.07	0.52	75	26 + 27	−57299 ± 207	0.37	0.61	75	26 + 27	−57097 ± 229	0.05	0.27
	33	−57175 ± 208	0.19	0.37		33	−57327 ± 225	−0.16	0.35		33	−57143 ± 241	0.20	0.09
	34	−57349 ± 184	0.74	0.07		34	−57507 ± 189	0.80	0.06		34	−57242 ± 208	0.75	0.02
	mean	−57302 ± 182				mean	−57461 ± 188				mean	−57215 ± 204		
74	31	−51901 ± 410	0.72	0.05	74	31	−52097 ± 421	0.72	0.05	74	31	−51774 ± 338	0.72	0.04
	32	−51567 ± 598	0.28	0.16		32	−51759 ± 603	0.28	0.16		32	−51467 ± 555	0.28	0.13
	mean	−51809 ± 369				mean	−52002 ± 379				mean	−51689 ± 385		
										82	19^a	−76283 ± 138	0.19	1.59
											22^a	−76448 ± 167	0.04	4.12
											23^a	−76045 ± 71	0.76	0.81
											mean	−76109 ± 180		

^{a} Sequences including ^{82}Rb.

$$\sigma^2(Y) = \left(\sum_p \nu_p \left\{\sigma_\pi(Y) + \sum_\alpha \frac{\partial M_p(Y)}{\partial M(\alpha)}\sigma(\alpha) + \sum_X \frac{\partial M_p(Y)}{\partial M(X)}\left[\sum_r \mu_r\left(\sigma_\rho(X) + \sum_\alpha \frac{\partial M_r(X)}{\partial M(\alpha)}\sigma(\alpha)\right)\right]\right\}\right)^2 ,$$

where again all crossed terms between different σ are zero. Using this equation, the weights ν_p may be determined as described in Eqs. (A9). Such a complete calculation takes into account the propagation of the errors through the successive measurements and the correlations (due to reference masses) between some of them. In particular this means that in the uncertainty $\sigma(X)$ on a measurement are included the uncertainties on the Table reference masses and the uncertainties on the preceding measurements.

APPENDIX B

The sequences using ^{82}Rb gave rise to dispersed results so that the experimental data on neutron-deficient rubidium isotopes have been processed following different assumptions:

(1) ^{82}Rb has the Atomic Mass Table [14] mass value.

(2) ^{82}Rb has the mass measured from the sequence 11 (80–82–83) first intended to be a test sequence, ^{80}Rb and ^{83}Rb having Atomic Mass Table[14] mass value.

(3) The mass of ^{82}Rb is supposed to be unknown and determined by the 3 sequences $N°$ 19, 22, 23 which included it.

The results are presented in Table IX. If assuming the third hypothesis, and calculating the ^{82}Rb mass from the measurements of the 3 sequences, the mean value obtained shows that the hypothesis 2 can be adopted which does not mean necessarily that the ^{82}Rb Table mass is wrong but that at least our measurement includes the ground state and the isomer masses. The mass of the isomer ^{82m}Rb is known but its proportion relative to the ground state at ISOLDE is not known.

*Present address: Gesellschaft für Schwerionen-forschung, 6100, Darmstadt, Germany.

†Permanent address: II. Physikalisches Institut, 6300 Giessen, Germany.

[1]1975 Mass Predictions, At. Data Nucl. Data Tables 17, Nos. 5–6 (1976) and references quoted therein.

[2]C. Thibault, R. Klapisch, C. Rigaud, A. M. Poskanzer, R. Prieels, L. Lessard, and W. Reisdorf, Phys. Rev. C 12, 644 (1975).

[3]X. Campi, H. Flocard, A. K. Kerman, and S. Koonin, Nucl. Phys. A251, 193 (1975).

[4]Atomic Masses and Fundamental Constants, Proceedings of the Fifth International Conference on Atomic Masses, edited by J. H. Sanders and A. H. Wapstra (Plenum, London, 1976).

[5]W. H. Johnson, Jr., Proceedings of the International Conference on the Properties of Nuclei far from the region of β stability, Leysin, 1970, CERN Report No. 70-30, 1970 (unpublished), p. 967.

[6]H. L. Ravn, S. Sundell, and L. Westgaard, Nucl. Instrum. Methods 123, 131 (1975).

[7]H. L. Ravn, Nucl. Instrum. Methods 139, 281 (1976).

[8]L. C. Carraz, I. R. Haldorsen, H. L. Ravn, M. Skarestad, and L. Westgaard, Nucl. Instrum. Methods 148, 217 (1978).

[9]H. L. Ravn, L. C. Carraz, J. Denimal, E. Kugler, M. Skarestad, S. Sundell, and L. Westgaard, Nucl. Instrum. Methods 139, 167 (1976).

[10]Mass Spectrometer Thomson CSF No. TSN 218.

[11]F. Touchard, G. Huber, R. Fergeau, C. Thibault, and R. Klapisch, Nucl. Instrum. Methods 155, 449 (1978).

[12]F. Touchard, Thèse de 3ème cycle, Université de Paris 7, 1977 (unpublished).

[13]W. F. G. Swann, J. Franklin Inst. 212, 439 (1931).

[14]A. H. Wapstra and K. Bos, At. Data Nucl. Data Tables 19, 175 (1977).

[15]J. M. D'Auria, L. C. Carraz, P. G. Hansen, B. Jonson, S. Mattsson, H. L. Ravn, M. Skarestad, and L. Westgaard, Phys. Lett. 66 B, 233 (1977).

[16]I. S. Towner, J. C. Hardy, and M. Harvey, Nucl. Phys. A 284, 269 (1977).

[17]D. H. Wilkinson, Phys. Lett. 67B, 13 (1977).

[18]ABMR experiment, C. Ekström, private communication to M. Epherre.

[19]A. H. Wapstra and N. B. Gove, Nucl. Data Tables 9, 265 (1971).

[20]A. H. Wapstra and K. Bos, At. Data Nucl. Data Tables 17, 474 (1976).

[21]S. Liran and N. Zeldes, Report No. IDKA 75/14 of the Institut für Kernphysik, Technische Hochschule, Darmstadt (unpublished) and At. Data Nucl. Data Tables 17, 431 (1976).

[22]J. Jänecke, At. Data Nucl. Data Tables 17, 455 (1976).

[23]E. Comay and I. Kelson, At. Data Nucl. Data Tables 17, 463 (1976).

[24]J. Jänecke and B. P. Eynon, At. Data Nucl. Data Tables 17, 467 (1976).

[25]P. A. Seeger and W. M. Howard, Report No. LA-5750, Los Alamos Scientific Laboratory, 1974 (unpublished); Nucl. Phys. A238, 491 (1975), At. Data Nucl. Data Tables 17, 428 (1976).

[26]W. D. Myers, Droplet Model of Atomic Nuclei (Plenum, New York, 1977) and At. Data Nucl. Data Tables 17, 411 (1976).

[27]K. Takahashi, H. V. Groote, and E. R. Hilf, Report No. IKDA 76/26 of the Institut für Kernphysik, Technische Hochschule, Darmstadt (unpublished) and H. V. Groote, E. R. Hilf, and K. Takahashi, At. Data Nucl.

Data Tables 17, 418 (1976).

[28] W. D. Myers and W. J. Swiatecki, Nucl. Phys. 81, 1 (1966).

[29] S. G. Nilsson and O. Prior, K. Dan. Vidensk. Selsk. Mat. Fys. Medd. 32, No. 16 (1961).

[30] N. Zeldes, A. Grill, and A. Simievic, K. Dan Vidensk. Selsk. Mat. Fys. Skr. 3, No. 5 (1967).

[31] H. E. Duckworth, R. C. Barber, P. Van Rookhuysen, J. D. MacDougall, W. McLatchie, S. Whineray, R. L. Bishop, J. O. Meredith, P. Williams, G. Southon, W. Wong, B. G. Hogg, and M. E. Kettner, Phys. Rev. Lett. 23, 592 (1969).

[32] E. Cheifetz and J. B. Wilhelmy, in *Nuclear Spectroscopy and Reactions*, part C, edited by J. Cerny (Academic, New York, 1974), p. 229 and references quoted therein.

[33] N. Kaffrell, G. Franz, G. Klein, K. Sümmerer, G. Tittel, N. Trautmann and G. Herrmann, in Proceedings of the 3rd International Conference on nuclei far from stability, Cargèse, (1976), CERN Report No. CERN 76-13, 1976 (unpublished), p. 483.

[34] H. Wollnik, F. K. Wohn, K. D. Wünsch, and G. Jung, Nucl. Phys. A291, 355 (1977).

[35] R. C. Jared, H. Nifenecker, and S. G. Thompson, in *Proceedings of the Third IAEA Symposium on the Physics and Chemistry of Fission, Rochester, 1973* (IAEA, Vienna, 1974), Vol. II, p. 211.

[36] R. G. Clark, L. E. Glendenin, W. L. Talberg, in *Proceedings of the Third IAEA Symposium on the Physics and Chemistry of Fission, Rochester, 1973* (IAEA, Vienna, 1974), Vol. II, p. 221.

[37] S. A. E. Johansson, Nucl. Phys. 64, 147 (1965).

[38] J. W. Grüter, K. Sistemich, P. Armbruster, J. Eidens, and H. Lawin, in Proceedings of the International Conference on the Properties of Nuclei far from the region of β-stability, Leysin, 1970, (CERN Report No. CERN 70-30, 1970 (unpublished), p. 967.

[39] T. A. Khan, D. Hofmann, and F. Horsch, Nucl. Phys. A205, 488 (1973).

[40] T. A. Khan, W. D. Lauppe, G. Salder, H. A. Selic, H. Lawin, and K. Sistemich, in Proceedings of the Third International Conference on Nuclei far from Stability, Cargèse, 1976 (see Ref. 33), p. 488.

[41] D. A. Arseniev, A. Sobiczewski, and V. G. Soloviev, Nucl. Phys. A139, 269 (1969).

[42] I. Ragnarsson, A. Sobiczewski, R. K. Sheline, S. E. Larsson, and B. Nerlo-Pomorska, Nucl. Phys. A233, 329 (1974).

[43] H. J. Krappe, J. R. Nix, in *Proceedings of the IAEA Symposium on the Physics and Chemistry of Fission, Rochester, 1973* (IAEA, Vienna, 1974), Vol. I, p. 159.

[44] G. Gneuss and W. Greiner, Nucl. Phys. A171, 449 (1971).

[45] A. Faessler, J. E. Galonska, U. Götz, and H. C. Pauli, Nucl. Phys. A230, 302 (1974).

[46] R. K. Sheline, I. Ragnarsson, and S. G. Nilsson, Phys. Lett. 41B, 115 (1972).

[47] R. K. Sheline, in Proceedings of the 3rd International Conference on Nuclei far from Stability, Cargèse, (1976) (see Ref. 33), p. 351.

[48] C. Ekström, S. Ingelman, G. Wannberg, and M. Skarestad, Nucl. Phys. A292, 144 (1977); C. Ekström, G. Wannberg, and J. Heinemeier, Phys. Lett. 76B, 565 (1978).

[49] J. Genevey-Rivier, A. Charvet, G. Marguier, C. Richard-Serre, J. D'Auria, A. Huck, G. Klotz, A. Knipper, and G. Walter, Nucl. Phys. A283, 45 (1977).